Novel validation of a 3D nonlinear finite element head-neck model for kinematical applications

Dávid Danka[1]*, Péter Szloboda[2], Imre Bojtár[1]

[1] Department of Structural Mechanics, Faculty of Civil Engineering, Budapest University of Technology and Economics, Hungary

[2] Department of Neurosurgery, St. John Hospital, Hungary

DOI: 10.17489/biohun/2022/2/367

Abstract

Computational biomechanical models have the potential to broaden our understanding and to aid the work of many practicing medical professionals. However, these models are only reliable, thus applicable and valuable, insofar as they are able to replicate a specific portion of reality. Therefore, validation of computational models is indispensable. To ensure that our proposed 3D finite element head-neck model does bear meaningful resemblance to real cervical spines, we relied on all available relevant rotation-moment measurements. Previously proposed validation metrics were used to quantify model error and experimental uncertainties. These metrics may be adopted for a wide range of other applications as well. Our model was found to be adequate for the study of kinematical properties of the human cervical spine.

Keywords: finite element model; cervical spine; head-neck complex; validation; rotation-moment relationship;

Introduction

Numerical studies of the human cervical spine are of great importance for several reasons. One of the most important one is that computational models allow us to obtain quantitative data that otherwise would be impossible to be obtained. However, a well-known problem arises: the model's ability to replicate realistic results for a specific application has to be investigated otherwise the simulation model cannot be relied on. In short, validation is of paramount importance.

Although numerical studies of the cervical spine do begin with validation, the usually applied methods are far from comprehensive and adequately quantitative. In numerous studies[1–14], the ranges of motion or the rotations at a given moment magnitude of the simulation models were compared to that of in vitro and in silico models. In other words, merely singular data points were taken into account, not the whole rotation-moment relationship of each FSU.

***Corresponding author contact data:** Department of Structural Mechanics, Faculty of Civil Engineering, Budapest University of Technology and Economics, Műegyetem rkp. 3., H-1111 Budapest, Hungary **E-mail:** danka.david@emk.bme.hu **Tel.:** +36 20 382-3399

Citation: *Danka D, Szloboda P, Bojtár I. Novel validation of a 3D nonlinear finite element head-neck model for kinematical applications. Biomech Hung. 2022; 15(2):31-42.*

Received: 09/09/2022 **Accepted:** 09/12/2022

Furthermore, the severely restricted use of empirical observations is apparent. Most authors took advantage of only one or two sets of experimental kinematical data. In addition, the level of coincidence of the results are predominantly qualitatively described. For instance, a common phrase, with different variations, is the following: *"The results of the proposed model are in good agreement with empirical data."* Here, *"good agreement"* often lacks a clear, quantitative characterization in published works. As a result, assessing the improvement of biofidelity of subsequent models developed for similar applications is largely hindered.

A better approach to validation is the use of the two standard deviation wide range of experimental mean.[3–5,9,15] The corridor defined this way is conveniently established in view of the fact that standard deviation of observational data is almost universally provided. Besides, the corridor is more useful for a comprehensive validation of FSUs of simulation models since not merely the end points but also the progression of the rotation-moment relationship is taken into account. Hence, one can observe the behavior of the cervical segments in function of the applied moment. However, this approach allows us to assess biofidelity only in more of a qualitative sense as the extent of deviation from the observational mean might be described as either greater or less than the standard deviation. No further distinctions can be drawn numerically. Moreover, one cannot freely choose the confidence level at which the results are evaluated: only a static empirical corridor is given.

Besides, the uncertainty of the utilized experimental data is rarely compared to the model error in a quantitative sense. This aspect of the available measurement data should be seen as all-important because the reliability of the validation ought to be assessed in light of the observational uncertainties. On the other hand, parametric studies provide some insight into the above mentioned problem.[2,16–19] The work of Wei et al.[20] and Bredbenner et al.[21] constitutes noteworthy exceptions with regards to measuring finite element model error. In both studies, agreement with empirical data is quantified. Bredbenner et al. conducted a thorough stochastic analysis of both the observational data and the finite element results.

In the current study, our objective was to validate a head-neck finite element model with all available rotation-moment measurements by quantifying model error and empirical uncertainties using a relatively simple and intuitive method.

Methods

Finite element model

The finite element model that was previously developed and reported by Danka et al.[22] is hereby validated. *Figure 1* shows the lateral view of the whole simulation model. It is im-

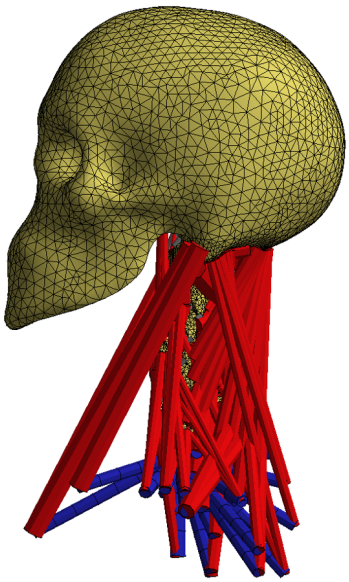

Figure 1. The previously developed finite element model of the human cervical spine[22]

portant to emphasize that muscles were not taken into account when the model was validated. In addition, a few adjustments detailed below were made. For further information, refer to the work of Danka et al.[22]

Some of the material model parameters, shown in *Table 1*, has been changed compared to the previously reported values. For the sake of completeness, all material constants are provided. In addition, the mechanical behavior of ligaments was more realistically taken into account. Ligaments' response due to tensile forces may be divided into three region, namely: toe region, elastic region and the plastic or failure region. The first two stages were captured using a quasi-bilinear approach. Ligaments were modeled by using tension-only truss elements. Besides, a fictive thermal load is applied so that the ligaments become compressed before applying moment loads. Hence, ligament laxity is taken into account. The work of Laville et al.[16] and Maurell et al.[23] were used as starting points to approximate the level of pre-slackening of each ligament. The applied initial strains by using fictive thermal loads are located in *Table 2*.

Table 1. Applied material constants

Anatomical part	Young's modulus [MPa]	Poisson's ratio [-]
Anterior Atlantoaxial Membrane	8	0.3
Anterior Atlantooccipital Membrane	1	0.3
Alar Ligament	5	0.3
Anterior Longitudinal Ligament	54.5	0.39
Apical Odontoid Ligament	20	0.3
Capsular Ligament	2	0.39
Interspinous Ligament	1.5	0.39
Intertransverse Ligament	2	0.39
Intervertebral Disk	3.4	0.39
Ligamentum Flavum	1.5	0.39
Muscle	1	0.4
Posterior Atlantoaxial Membrane	10	0.3
Posterior Atlantooccipital Membrane	20	0.3
Posterior Longitudinal Ligament	30	0.39
Bone	18000	0.4
Supraspinous Ligament	1.5	0.3
Transverse Ligament	20	0.3
Tectorial Membrane	10	0.3

Experimental datasets

The basis for empirical kinematical data was a meta-analysis study conducted by Zhang et al.[24] For this meta-analysis, numerous measurement results were collected and compiled. The compiled results that were used in the present work is located in the spreadsheet file of *Supplementary data 2 in Appendix A* of Zhang et al.'s paper. The inclusion criteria of our study were defined as follows. Datasets that (1) include at least one cervical FSU, (2) were produced with no follower load or compressive force, and (3) provide at least two data points per loading directions were taken into account. If datasets were only available for unilateral moments, in case of LB and AR, then

Table 2. Applied initial compressive strain in ligaments

Ligament	Compressive strain [%]
Anterior Longitudinal Ligament	-10
Posterior Longitudinal Ligament	-10
Capsular Ligament	-30
Interspinous Ligament	-17
Supraspinous Ligament	-10
Anterior Atlantooccipital Membrane	-10
Anterior Atlantoaxial Membrane	-10
Posterior Atlantooccipital Membrane	-10
Posterior Atlantoaxial Membrane	-10

the results were assumed to be the same due to contralateral moments with opposite sign.

Loads and boundary conditions

In order to validate the model, prescribed rotations were applied at the top of the skull (see *Figure 2*). In all simulations, fixed support boundary condition was defined at the bottom surface of the C7 vertebral body. Since the observational data are derived from intact cervical spine specimens without muscle tissue, muscles in the finite element model were suppressed thus not taken into account. ANSYS's[25] *Remote Point* feature was utilized to measure the rotation. The *Remote Points* were placed onto the anterior surface of the vertebral bodies. In the post-processing stage, the *Flexible Rotation* result object provided the rotation values of each vertebra.

Validation metrics

In order to quantify the biofideliy of the finite element model, validation metrics proposed by Oberkampf and Barone[26] were used. A brief description of each validation metric is presented below. For further details and rigorous derivation of each metric, refer to the work of Oberkampf and Barone.[26]

Here, a list of the quantities occurring in the following equations is provided:

- M – applied moment,
- M_u and M_l – maximum and minimum value of the applied moment, respectively,
- $\theta_m(M)$ – relative rotations of a specific FSU in the proposed FE model,
- $\overline{\theta}_c(M)$ – mean relative rotations of human cervical spine samples for a specific FSU,
- $\widetilde{E}(M)$ – estimated error function, $\widetilde{E}(M) = \theta_m(M) - \overline{\theta}_c(M)$
- $s(M)$ – standard deviation of mean relative rotations,
- C – confidence level,
- α – total area of both of the tails of the probability density function of Student's t-distribution,
- $n(M)$ – number of independent dataset for a given moment magnitude,
- $v(M)$ – degree of freedom of the t-distribution, $v(M)=n(M)-1$.

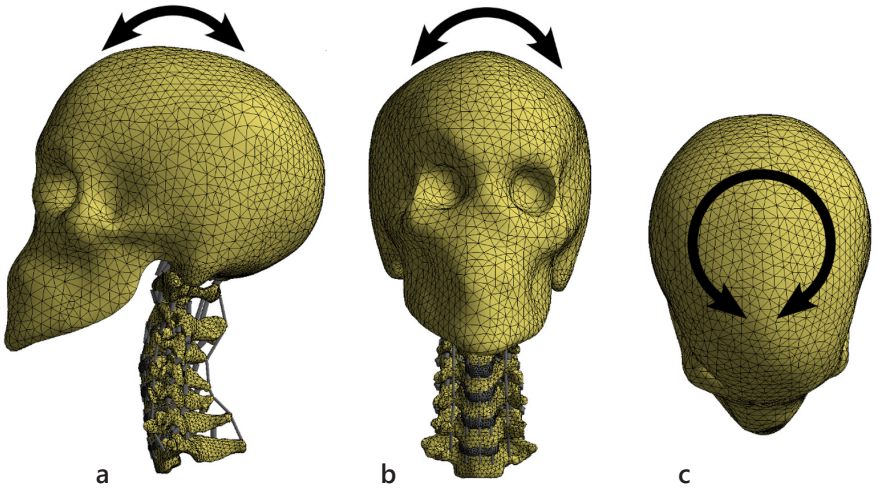

Figure 2. Application of prescribed rotation in all three loading direction: flexion-extension (a), lateral bending (b), axial rotation (c)

There are some basic mathematical restrictions that has to be respected in order to use the validation metrics introduced below. Both θ_m and $\bar{\theta}_e$ are required to be functions of M, i.e., one and only one relative rotation value can be assigned to each value of M. In addition, the value of $\bar{\theta}_e$ is not allowed to be 0 otherwise division by 0 occurs.

The first validation metric is the so called *average relative error metric* (AREM), which characterizes the absolute relative difference between measurements and the corresponding results of the computational model. This validation metric is calculated as follows *(1)*:

$$AREM = \frac{1}{(M_u - M_l)} \int_{M_l}^{M_u} \left| \frac{\theta_m(M) - \bar{\theta}_e(M)}{\bar{\theta}_e(M)} \right| dM \quad (1)$$

The *average relative confidence indicator* (ARCI) is defined as the average magnitude of the half-width of the confidence interval over the range of the applied moment *(2)*:

$$ARCI = \frac{1}{(M_u - M_l)} \int_{M_l}^{M_u} \frac{t_{\alpha/2,v}(M)}{\sqrt{n(M)}} \left| \frac{s(M)}{\bar{\theta}_e(M)} \right| dM \quad (2)$$

The *maximum relative error metric* (MREM) is simply the maximum value of the absolute relative error over the range of the applied moment *(3)*:

$$MREM = \max_{M_l \le M \le M_u} \left| \frac{\theta_m(M) - \bar{\theta}_e(M)}{\bar{\theta}_e(M)} \right| \quad (3)$$

Let $\hat{M}$ denote the moment magnitude at which MREM occurs. Then the *maximum relative confidence interval* (MRCI) is the half of the relative confidence interval at $\hat{M}$ *(4)*:

$$MRCI = \frac{t_{\alpha/2,v}(\hat{M})}{\sqrt{n(\hat{M})}} \left| \frac{s(\hat{M})}{\bar{\theta}_e(\hat{M})} \right| \quad (4)$$

Moreover, validation metrics that are continuous functions of M are introduced. The rationale behind the application of these additional metrics is the need to compare the empirical and finite element results more thoroughly. The confidence interval around the experimental mean *(5)* and around the estimated error *(6)*, the relative confidence interval around the absolute relative estimated error *(7)*, respectively, are defined as follows:

$$I_e(M) = \left(\bar{\theta}_e(M) - t_{\alpha/2,v}(M) \frac{s(M)}{\sqrt{n(M)}}, \bar{\theta}_e(M) + t_{\alpha/2,v}(M) \frac{s(M)}{\sqrt{n(M)}} \right) \quad (5)$$

$$I_{\tilde{E}}(M) = \left(\tilde{E}(M) - t_{\alpha/2,v}(M) \frac{s(M)}{\sqrt{n(M)}}, \tilde{E}(M) + t_{\alpha/2,v}(M) \frac{s(M)}{\sqrt{n(M)}} \right) \quad (6)$$

$$I_{\tilde{E},rel}(M) = \left(\left| \frac{\tilde{E}(M)}{\bar{\theta}_e(M)} \right| - \frac{t_{\alpha/2,v}(M)}{\sqrt{n(M)}} \left| \frac{s(M)}{\bar{\theta}_e(M)} \right|, \left| \frac{\tilde{E}(M)}{\bar{\theta}_e(M)} \right| + \frac{t_{\alpha/2,v}(M)}{\sqrt{n(M)}} \left| \frac{s(M)}{\bar{\theta}_e(M)} \right| \right) \quad (7)$$

Validation procedure

First, the results of the finite element model were extracted, i.e., the moment reaction due to the prescribed rotation and the absolute rotation of each vertebral body. Absolute angulations were converted into relative ones simply by subtracting absolute rotations of one vertebra from absolute rotations of the adjacent, superior vertebra.

Furthermore, empirical data had to be compiled as well, although minor modifications were sufficient. In the following, the most notable adjustments and assumptions are mentioned. The experimental datasets do

not satisfy the criteria above at all input values, that is, more than one relative rotation value is assigned to certain moment magnitudes. In observational studies, the end point values of the neutral zone were assigned to $M = 0$ Nm moment. Thereby, two distinct relative rotation values are designated to one M instead of one. To address this issue, neutral zone end point angulations were assigned to $M = +0.02$ Nm and $M = -0.02$ Nm. These moment magnitudes are close enough to 0 from a practical point of view but not too close from a numerical perspective.

In addition, no initial angulation was assumed therefore $\theta = 0°$ was assigned to $M = 0$ Nm in case of each motion segment. However, this presumption poses another problem: when calculating some of the above mentioned metrics, one must divide by 0. This issue is resolved by proposing that the relative error and relative confidence interval is 0% at $M = 0$ Nm. With these assumptions and preprocessing, $C = 95\%$ confidence level was chosen, thus $\alpha = 5\%$, and the validation metrics were calculated interpolating between data points of each empirical and finite element rotation-moment result set.

Results

Utilized empirical datasets

Altogether 9 observational studies were found to meet the inclusion criteria. Each report provides kinematical data of various cervical spine segments, therefore it is useful to show the distribution of available experimental data in *Figure 3* and *Table 3*. Since relatively few and varying number of datasets of FSUs are available in different loading directions, it follows that the length of the CI is largely influenced by the number of available datasets. Upper cervical spine segments in FE have the largest number of empirical datasets while these segments in LB and C2-C3 in FE have the least amount of observational datasets. The lower cervical spine is balanced in all free loading directions in this respect. It is worth noting that the only empirical study that reports on rotation-moment data of the six FSUs in all three loading direction was conducted by Panjabi et al.[27]

Global validation metric results

Results pertaining to global metrics are summarized in *Table 4* and in *Figure 4*. One may observe that, on average, the magnitude of relative error is larger in case of LB than that of FE and AR. The smallest and largest average relative error is associated with FE of C0-C1, being 12.5%±81.4% with 95% confidence and with LB of C1-C2, being 77.3%±125.9% with 95% confidence, respectively. The smallest and largest maximum relative error is related to AR of C1-C2 with 58.2%±100.3% with 95% confidence and to LB of C1-C2, being 156.8%±85.8% with 95% confidence.

One of the most prominent patterns in the results is that the lengths of relative confi-

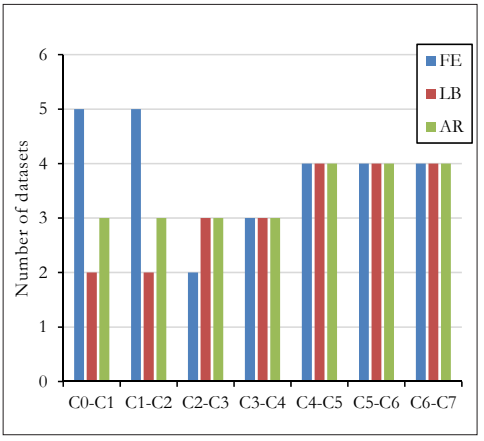

Figure 3. Number of used independent datasets for each FSU and for each loading direction

Table 3. Utilized empirical datasets for each motion segment and for each loading direction

Motion segment	FE	LB	AR
C0C1	Panjabi et al.[27] Panjabi et al.[28] Kettler et al.[29] Nightingale et al.[30] Nightingale et al.[31]	Panjabi et al.[27] Panjabi et al.[28]	Panjabi et al.[27] Panjabi et al.[28] Kettler et al.[29]
C1C2	Panjabi et al.[27] Panjabi et al.[28] Kettler et al.[29] Nightingale et al.[30]	Panjabi et al.[27] Panjabi et al.[28]	Panjabi et al.[27] Panjabi et al.[28] Kettler et al.[29]
C2C3	Panjabi et al.[27] Wheeldon et al.[32]	Panjabi et al.[27] Yoganandan et al.[33] Yoganandan et al.[34]	Panjabi et al.[27] Yoganandan et al.[33] Yoganandan et al.[34]
C3C4	Panjabi et al.[27] Nightingale et al.[30] Wheeldon et al.[32]	Panjabi et al.[27] Yoganandan et al.[33] Yoganandan et al.[34]	Panjabi et al.[27] Yoganandan et al.[33] Yoganandan et al.[34]
C4C5	Panjabi et al.[27] Nightingale et al.[31] Wheeldon et al.[32] Bozkus et al.[35]	Panjabi et al.[27] Yoganandan et al.[33] Yoganandan et al.[34] Bozkus et al.[35]	Panjabi et al.[27] Yoganandan et al.[33] Yoganandan et al.[34] Bozkus et al.[35]
C5C6	Panjabi et al.[27] Nightingale et al.[30] Wheeldon et al.[32] Bozkus et al.[35]	Panjabi et al.[27] Yoganandan et al.[33] Yoganandan et al.[34] Bozkus et al.[35]	Panjabi et al.[27] Yoganandan et al.[33] Yoganandan et al.[34] Bozkus et al.[35]
C6C7	Panjabi et al.[27] Nightingale et al.[31] Wheeldon et al.[32] Bozkus et al.[35]	Panjabi et al.[27] Yoganandan et al.[33] Yoganandan et al.[34] Bozkus et al.[35]	Panjabi et al.[27] Yoganandan et al.[33] Yoganandan et al.[34] Bozkus et al.[35]

Table 4. Global validation metric results for each loading direction and motion segment

Motion type	Motion segment	AREM	ARCI	MREM	MRCI
FE	C0-C1	12.5%	81.4%	83.1%	444.5%
	C1-C2	22.4%	69.2%	63.3%	111.5%
	C2-C3	35.1%	316.4%	95.2%	846.9%
	C3-C4	27.5%	108.6%	101.9%	312.8%
	C4-C5	21.1%	104.3%	115.2%	205.8%
	C5-C6	40.3%	88.8%	118.0%	195.6%
	C6-C7	17.6%	76.7%	126.2%	200.7%
LB	C0-C1	39.4%	179.2%	61.8%	267.5%
	C1-C2	77.3%	125.9%	156.8%	85.8%
	C2-C3	44.8%	145.5%	97.5%	92.3%
	C3-C4	34.7%	80.4%	99.1%	60.6%
	C4-C5	54.1%	78.7%	100.8%	104.9%
	C5-C6	34.8%	69.1%	103.0%	102.3%
	C6-C7	43.5%	111.9%	103.9%	117.8%
AR	C0-C1	40.4%	140.8%	86.4%	94.0%
	C1-C2	24.8%	111.4%	58.2%	100.3%
	C2-C3	24.1%	75.9%	86.8%	37.2%
	C3-C4	33.3%	109.2%	90.9%	97.6%
	C4-C5	45.5%	80.1%	91.3%	106.3%
	C5-C6	23.2%	97.9%	84.7%	113.7%
	C6-C7	19.9%	96.8%	79.4%	121.1%

dence intervals are considerably greater than the magnitude of the corresponding relative error. The smallest (37.2%) and largest MRCI (846.9%) is accompanied to the case of AR and FE of C2-C3, respectively. Upon inspection of relative CI in the function of moment, relative errors came to be largest near the initial position and at the ends of rotation-moment curves.

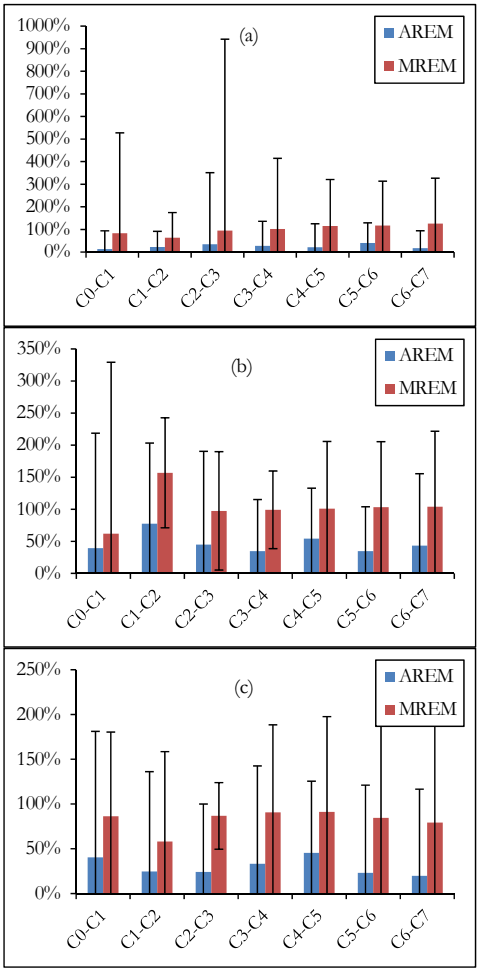

Figure 4. Global validation metrics with error bars showing the corresponding ARCI and MRCI. The graphs show the results derived from flexion-extension (a), lateral bending (b) and axial rotation (c) loading directions

Continuous confidence intervals, error and relative error

In this section, results of FSUs having the smallest (*Figure 5*) and largest (*Figure 6*) average relative error are detailed. The agreement between rotation-moment behavior of C0-C1 due to FE with corresponding empirical results is the greatest. Both ends of the neutral zone are practically coincident with the observational mean. The biofidelity in flexion is excellent as well as in extension until -1 Nm moment magnitude. The measurements signal a stiffening behavior while the finite element model response remains mostly linear. However, not only the magnitude of error and relative error rises but the length of the corresponding confidence interval does as well. This pattern is typical of numerous result sets as well as the fact that a local or even the global maximum relative error occurs near the initial position.

As far as the worst performing FSU is concerned (*Figure 6*), most of the average error stems from the fact that the one of the ends of neutral zone is not captured precisely. Regardless, the slope of the rotation-moment curve of the FEM is roughly the same as that of the experimental mean in the elastic zone. Furthermore, the FEM rotation-moment curve is not entirely out of the CIs although the CIs were determined by merely two set of observational measurements (*Figure 3*), meaning that they prone to change significantly if newer observational data would be added as input to the calculation of validation metrics. For further details on continuous validation metrics of other FSUs, please refer to the supplementary materials.

Discussion

Novelties

To the authors' knowledge, this is the first study that not only quantified computational

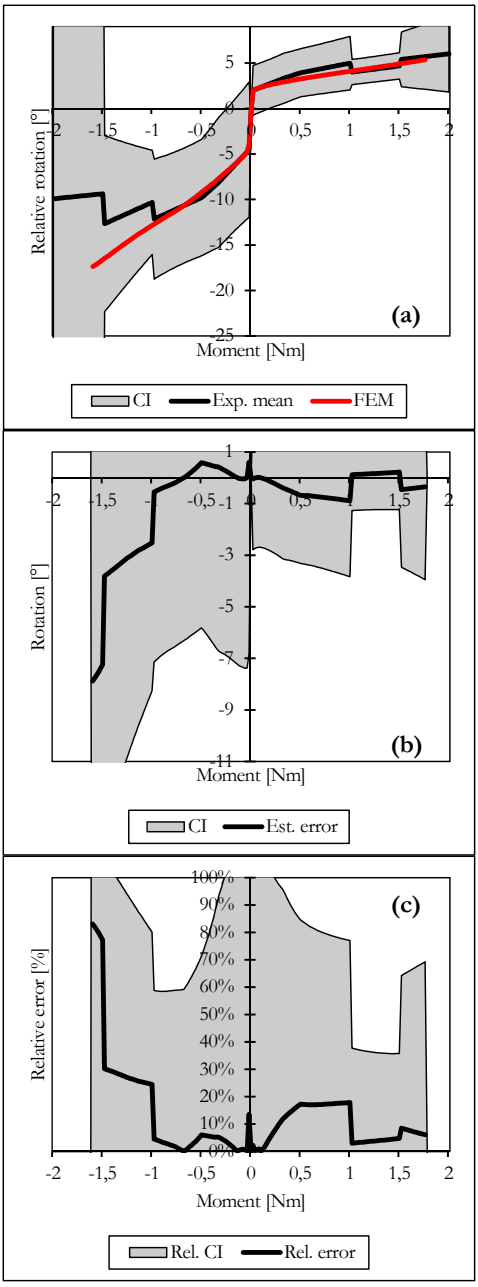

Figure 5. Continuous validation metrics pertaining to FE of C0-C1: experimental mean with confidence interval compared to FEM result (a), estimated error with confidence interval (b), absolute relative error with relative confidence interval (c)

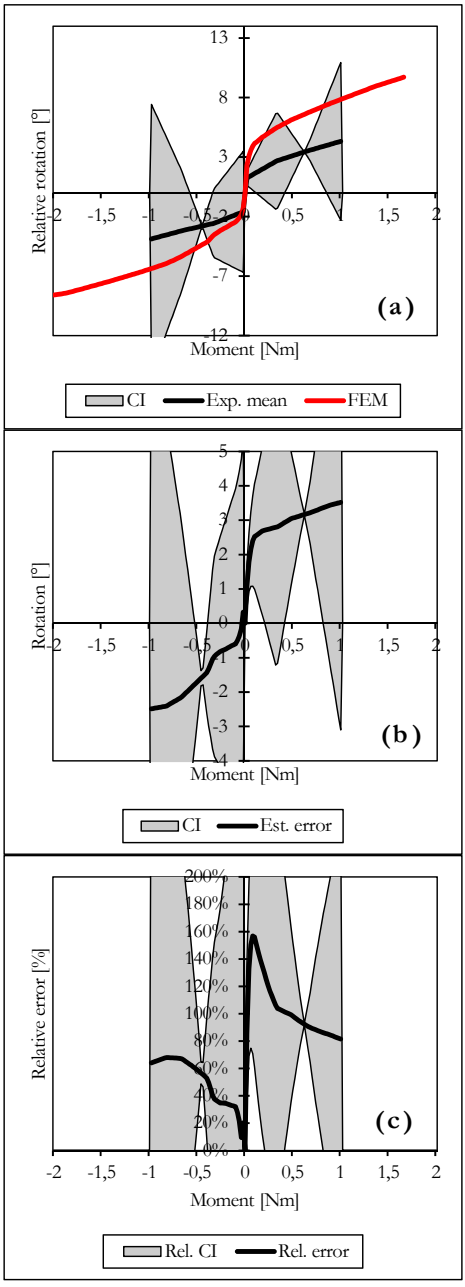

Figure 6. Continuous validation metrics pertaining to LB of C1-C2: experimental mean with confidence intervals compared to FEM results (a), estimated error with confidence intervals (b), absolute relative errors with relative confidence intervals (c)

model error of the cervical spine but reports on the structure of uncertainty of the rotation-moment experimental data as well. This information is of great importance since rotation-moment data are widely used for validating computational spine models. Moreover, the stochastic analysis was carried out taking advantage of all available rotation-moment measurements, which means that results of 9 studies were utilized.

Another novelty is the use of a specific set of validation metrics that, as far as the authors are aware, has not been applied to human cervical spine computational models before. However, these metrics provide a relatively easy and intuitive use of the available empirical data. Besides, the presented validation metrics allow us in the future to compare different finite element models of the cervical spine. Incorporating future measurements and reassessing model performance is also possible with little effort. Consequently, it provides a consistent and quantitative framework. The presented validation metrics may also be successfully applied in a wide variety of validation problems. Although with moderate limitations, even comparisons between computational models of different anatomical parts are also possible with regards to biofidelity.

Limitations

One major drawback of the present study is the dataset itself, which the stochastic analysis was based on. Firstly, the number of the empirical studies of the cervical spine is relatively few. Ideally, for each FSU and for each loading direction at least 15-30 observational rotation-moment datasets is needed to reduce the confidence intervals significantly. Secondly, multi-segment cervical spine rotation-moment data are reported mostly instead of uni-segment data. This led Zhang et al.[24] to make approximations in order to acquire kinematical data for individual spinal units. Clearly, this is one additional source of uncertainty.

It is well-established that cervical motions are complex.[36] However, there is an even greater scarcity of data regarding the coupled motion patterns of the cervical spine. To the authors' knowledge, the only study that comprehensively reports data of such kind was conducted by Panjabi et al.[27] One improvement would be to validate the model not only against principal motions but also against secondary motions after sufficient amount of such data becomes available.

Another obvious weakness of this study is that the measurements were conducted mostly on elderly cadaveric spinal units. The proposed finite element model, on the other hand, was developed based on CT of a young, 21-year-old male. Furthermore, different magnitude of ultimate moments is applied in different experimental studies. The larger the ultimate moment is, the fewer sets of observational data there are. This is a major component of why the empirical uncertainties rise at both ends of the rotation-moment curve. For this reason, more measurements are needed. Another deficiency is that the muscles are not validated. There is no available data that considers the whole head-neck complex and provides rotation-moment curves.

Conclusion

In this research paper, a previously developed finite element model of the human cervical spine[22] was adjusted and validated. Both model error and empirical uncertainties with 95% confidence were quantified. The proposed finite element model was found to be adequate for kinematical applications such as range of motion comparisons of different surgical procedures or kinematical analysis of cervical spine injuries.

Author contributions: D.D. conducted the literature review, developed the FE model, ran the simulations, performed the validation, wrote the manuscript. S.P. gave feedback on the FE model results from a physiological perspective and suggested specific ways of how the model should be improved further. B.I. checked the results of the simulations and gave feedback on the manuscript.

Conflict of interest: None

Abbreviations: AR – axial rotation, CI – confidence interval, FE – flexion-extension, FEM – finite element model, FSU – functional spinal unit, LB – lateral bending

REFERENCES

1. *Manickam PS, Roy S.* The biomechanical study of cervical spine: A Finite Element Analysis. Int J Artif Organs. 2021 Mar 1;0391398821995495.
2. *Nikkhoo M, Cheng C-H, Wang J-L, et al.* Development and validation of a geometrically personalized finite element model of the lower ligamentous cervical spine for clinical applications. Computers in Biology and Medicine. 2019;109:22–32.
3. *Wang K, Deng Z, Wang H, Li Z, Zhan H, Niu W.* Influence of variations in stiffness of cervical ligaments on C5-C6 segment. J Mech Behav Biomed Mater. 2017;72:129–37.
4. *Rong X, Wang B, Ding C, et al.* The biomechanical impact of facet tropism on the intervertebral disc and facet joints in the cervical spine. The Spine Journal. 2017;17(12):1926–31.
5. *Östh J, Brolin K, Svensson MY, Linder A.* A female ligamentous cervical spine finite element model validated for physiological loads. J Biomech Eng. 2016 May 2;138(6):061005-061005–9.
6. *Toosizadeh N, Haghpanahi M.* Generating a finite element model of the cervical spine: Estimating muscle forces and internal loads. Scientia Iranica. 2011 Dec;18(6):1237–45.
7. *Kallemeyn N, Gandhi A, Kode S, Shivanna K, Smucker J, Grosland N.* Validation of a C2–C7 cervical spine finite element model using specimen-specific flexibility data. Med Eng Phys. 2010 Jun 1;32(5):482–9.
8. *Li Z, Song G, Su Z, Wang G.* Development, validation, and application of ligamentous cervical spinal segment C6-C7 of a six-year-old child and an adult. Computer Methods and Programs in Biomedicine. 2020;183:105080.
9. *Cai X-Y, Sang D, Yuchi C-X, et al.* Using finite element analysis to determine effects of the motion loading method on facet joint forces after cervical disc degeneration. Computers in Biology and Medicine. 2020 Jan 1;116:103519.
10. *Hua W, Zhi J, Wang B, et al.* Biomechanical evaluation of adjacent segment degeneration after one- or two-level anterior cervical discectomy and fusion versus cervical disc arthroplasty: A finite element analysis. Computer Methods and Programs in Biomedicine. 2020 Jun 1;189:105352.
11. *Herron MR, Park J, Dailey AT, Brockmeyer DL, Ellis BJ.* Febio finite element models of the human cervical spine. J Biomech. 2020;113:110077.
12. *Zhou E, Huang H, Zhao Y, Wang L, Fan Y.* The effects of titanium mesh cage size on the biomechanical responses of cervical spine after anterior cervical corpectomy and fusion: A finite element study. Clinical Biomechanics. 2022;91:105547.
13. *Li J, Gan K, Chen B, et al.* Anterior cervical transpedicular screw fixation system in subaxial cervical spine: A finite element comparative study. Medicine. 2022 Jul 22;101(29):e29316.
14. *Hua W, Zhi J, Ke W, et al.* Adjacent segment biomechanical changes after one- or two-level anterior cervical discectomy and fusion using either a zero-profile device or cage plus plate: A finite element analysis. Computers in Biology and Medicine. 2020 May 1;120:103760.
15. *Erbulut DU, Zafarparandeh I, Lazoglu I, Ozer AF.* Application of an asymmetric finite element model of the C2-T1 cervical spine for evaluating the role of soft tissues in stability. Med Eng Phys. 2014 Jul 1;36(7):915–21.

16. *Laville A, Laporte S, Skalli W.* Parametric and subject-specific finite element modelling of the lower cervical spine. Influence of geometrical parameters on the motion patterns. Journal of Biomechanics. 2009 Jul 22;42(10):1409–15.
17. *John JD, Saravana Kumar G, Yoganandan N.* Cervical spine morphology and ligament property variations: A finite element study of their influence on sagittal bending characteristics. J Biomech. 2019 Mar 6;85:18–26.
18. *Dogru SC, Arslan YZ.* Effect of model parameters on the biomechanical behavior of the finite element cervical spine model. Applied Bionics and Biomechanics. 2021 Jun 28;2021:e5593037.
19. *Komeili A, Rasoulian A, Moghaddam F, El-Rich M, Li LP.* The importance of intervertebral disc material model on the prediction of mechanical function of the cervical spine. BMC Musculoskelet Disord. 2021 Dec;22(1):324.
20. *Wei W, Liu Y, Du X, Li N.* Development and validation of a C0-C7 cervical spine finite element model. MATEC Web of Conferences. 2017;108:13007.
21. *Bredbenner TL, Eliason TD, Francis WL, McFarland JM, Merkle AC, Nicolella DP.* Development and validation of a statistical shape modeling-based finite element model of the cervical spine under low-level multiple direction loading conditions. Front Bioeng Biotechnol [Internet]. 2014 [cited 2019 Feb 12];2. Available from: *https://www.frontiersin.org/articles/10.3389/fbioe.2014.00058/full*
22. *Danka D, Szloboda P, Nyáry I, Bojtár I.* The fracture of the human cervical spine. Materials Today: Proceedings. 2022 Jun 24;62:2495–501.
23. *Maurel N, Lavaste F, Skalli W.* A three-dimensional parameterized finite element model of the lower cervical spine, study of the influence of the posterior articular facets. Journal of Biomechanics. 1997 Sep 1;30(9):921–31.
24. *Zhang C, Mannen EM, et al.* Moment-rotation behavior of intervertebral joints in flexion-extension, lateral bending, and axial rotation at all levels of the human spine: A structured review and meta-regression analysis. J Biomech. 2020 ;100:109579.
25. ANSYS 2021 R1. Canonsburg, Pennsylvania, USA: Ansys, Inc.; 2021.
26. *Oberkampf WL, Barone MF.* Measures of agreement between computation and experiment: Validation metrics. Journal of Computational Physics. 2006 Sep;217(1):5–36.
27. *Panjabi MM, Crisco JJ, Vasavada A, et al.* Mechanical properties of the human cervical spine as shown by three-dimensional load–displacement curves. Spine. 2001 Dec;26(24):2692–700.
28. *Panjabi M, Dvorak J, Duranceau J, et al.* Three-dimensional movements of the upper cervical spine. Spine. 1988 Jul;13(7):726–30.
29. *Kettler A, Hartwig E, Schultheiß M, Claes L, Wilke H-J.* Mechanically simulated muscle forces strongly stabilize intact and injured upper cervical spine specimens. J Biomech. 2002 Mar 1;35(3):339–46.
30. *Nightingale RW, Winkelstein BA, Knaub KE, Richardson WJ, Luck JF, Myers BS.* Comparative strengths and structural properties of the upper and lower cervical spine in flexion and extension. J Biomech. 2002 Jun;35(6):725–32.
31. *Nightingale RW, Carol Chancey V, Ottaviano D, et al.* Flexion and extension structural properties and strengths for male cervical spine segments. J Biomech. 2007 Jan 1;40(3):535–42.
32. *Wheeldon JA, Pintar FA, Knowles S, Yoganandan N.* Experimental flexion/extension data corridors for validation of finite element models of the young, normal cervical spine. J Biomech. 2006;39(2):375–80.
33. *Yoganandan N, Pintar FA, Stemper BD, Wolfla CE, Shender BS, Paskoff G.* Level-dependent coronal and axial moment-rotation corridors of degeneration-free cervical spines in lateral flexion. The Journal of Bone & Joint Surgery. 2007 May;89(5):1066–74.
34. *Yoganandan N, Stemper BD, Pintar FA, Baisden JL, Shender BS, Paskoff G.* Normative segment-specific axial and coronal angulation corridors of subaxial cervical column in axial rotation: Spine. 2008 Mar;33(5):490–6.
35. *Bozkus H, Ames CP, Chamberlain RH, et al.* Biomechanical analysis of rigid stabilization techniques for three-column injury in the lower cervical spine. Spine. 2005 Apr;30(8):915–22.
36. *Bogduk N, Mercer S.* Biomechanics of the cervical spine. I: Normal kinematics. Clin Biomech. 2000;16.